BJA

British Journal of Anaesthesia, 126 (6): 1141–1156 (2021)

doi: 10.1016/j.bja.2021.01.017
Advance Access Publication Date: 26 February 2021
Neuroscience and Neuroanaesthesia

Behavioural impairments after exposure of neonatal mice to propofol are accompanied by reductions in neuronal activity in cortical circuitry

Hang Zhou[1], Zhongcong Xie[2], Ansgar M. Brambrink[1] and Guang Yang[1,*]

[1]Department of Anesthesiology, Columbia University Irving Medical Center, New York, NY, USA and [2]Department of Anesthesia, Critical Care and Pain Medicine, Massachusetts General Hospital and Harvard Medical School, Charlestown, MA, USA

*Corresponding author. E-mail: gy2268@cumc.columbia.edu

This article is accompanied by an editorial: Anaesthesia, neural activity, and brain development: interneurones in the spotlight by L. Vutskits, *Br J Anaesth* 2021:126:1084–1085, doi: 10.1016/j.bja.2021.03.002

Abstract

Background: Both animal and retrospective human studies have linked extended and repeated general anaesthesia during early development with cognitive and behavioural deficits later in life. However, the neuronal circuit mechanisms underlying this anaesthesia-induced behavioural impairment are poorly understood.

Methods: Neonatal mice were administered one or three doses of propofol, a commonly used i.v. general anaesthetic, over Postnatal days 7–11. Control mice received Intralipid® vehicle injections. At 4 months of age, the mice were subjected to a series of behavioural tests, including motor learning. During the process of motor learning, calcium activity of pyramidal neurones and three classes of inhibitory interneurones in the primary motor cortex were examined *in vivo* using two-photon microscopy.

Results: Repeated, but not a single, exposure of neonatal mice to propofol i.p. caused motor learning impairment in adulthood, which was accompanied by a reduction of pyramidal neurone number and activity in the motor cortex. The activity of local inhibitory interneurone networks was also altered: somatostatin-expressing and parvalbumin-expressing interneurones were hypoactive, whereas vasoactive intestinal peptide-expressing interneurones were hyperactive when the mice were performing a motor learning task. Administration of low-dose pentylenetetrazol to attenuate γ-aminobutyric acid A receptor-mediated inhibition or CX546 to potentiate α-amino-3-hydroxy-5-methyl-4-isoxazolepropionic acid-subtype glutamate receptor function during emergence from anaesthesia ameliorated neuronal dysfunction in the cortex and prevented long-term behavioural deficits.

Conclusions: Repeated exposure of neonatal mice to propofol anaesthesia during early development causes cortical circuit dysfunction and behavioural impairments in later life. Potentiation of neuronal activity during recovery from anaesthesia reduces these adverse effects of early-life anaesthesia.

Keywords: anaesthetic neurotoxicity; behaviour; calcium; cerebral cortex; interneurone; propofol; pyramidal neurone

Editor's key points

- Repeated exposures to general anaesthesia during early development are associated with cognitive and behavioural deficits later in life in animal models, although the mechanisms are poorly understood.
- Propofol exposure in neonatal mice induces a prolonged reduction of cortical pyramidal neuronal activity that persists into the anaesthesia recovery period.
- Repeated, but not a single, exposure of neonatal mice to propofol impaired motor learning in adulthood, which was accompanied by reduced pyramidal neurone

Received: July 6, 2020; **Accepted:** 16 January 2021

© 2021 British Journal of Anaesthesia. Published by Elsevier Ltd. All rights reserved.
For Permissions, please email: permissions@elsevier.com

number and activity in the motor cortex, and local inhibitory interneurone networks were also altered.
- Potentiation of neuronal activity during recovery from anaesthesia reduced these adverse effects of early-life anaesthesia, suggesting a potential neuroprotective strategy.

Neuronal activity is fundamental for the proper formation of cortical circuits, and disturbing activity during early brain development can have a marked impact on neuronal network function. For example, in the developing visual system, spontaneous and visually evoked activities drive the maturation of visual circuits, and blockade of such activity causes permanent vision loss.[1,2] Pathological consequences of disturbing early network activity are also evident in fetal alcohol syndrome, where ethanol causes a prominent increase in neuronal apoptosis by increasing γ-aminobutyric acid A ($GABA_A$) receptor function.[3] Most of the drugs commonly used for anaesthesia and sedation in the operating theatre and the ICU are potent modulators of neuronal activity,[4,5] raising concern that these drugs could have undesired effects on brain development.[6] In fact, several large retrospective human studies have linked multiple exposures to anaesthesia and surgery within the first 3 yr of life with subsequent learning difficulties.[7–9] Moreover, compelling evidence from laboratory animals shows that anaesthetics and sedatives, depending on dose, duration, and timing of administration, can cause apoptotic neurodegeneration and a wide range of behavioural deficits,[10–16] including learning difficulties.[17,18]

How neuronal circuitry in the cortex is modified by repeated anaesthetic exposure and how it then contributes to learning deficits remain unknown. At the cellular level, anaesthesia exposure can cause structural and functional changes in cortical pyramidal neurones, including alterations in the density and dynamics of postsynaptic dendritic spines, dendritic arborisation, neuronal activity, and synaptic protein expression.[19–21] In addition to these changes in glutamatergic neurones, effects on the highly interconnected network of GABAergic interneurones may also contribute to cognitive impairment. For example, anaesthesia has been shown to impair the dendritic growth, survival, and differentiation of immature GABAergic cells.[22–24] Within the motor cortex, there is a large diversity of inhibitory interneurones, including somatostatin (SST)-, parvalbumin (PV)-, and vasoactive intestinal polypeptide (VIP)-expressing neurones.[25] These different types of interneurones migrate from subcortical origins during early development and target specific domains of pyramidal neurones or other interneurones, providing precise control of excitatory and inhibitory outputs and cortical network activity.[26] How these glutamatergic neurones and GABAergic interneurone populations are altered by anaesthetic exposure during early postnatal development and contribute to behavioural deficits and cortical dysfunction in adulthood are not known.

In this study, we investigated the changes of pyramidal neurones and three types of interneurones in adult motor cortex after exposure of neonatal mice to propofol, a general anaesthetic used for paediatric anaesthesia and sedation.[27] By imaging neuronal activity in young mice during anaesthesia and recovery and in adulthood, we identified cell-type specific changes in cortical neuronal networks associated with motor learning impairments after repeated propofol exposure. Our results showed that neonatal anaesthesia causes a marked reduction of neuronal activity in pyramidal neurones and in SST and PV interneurones in the mouse motor cortex. Administration of sub-convulsant doses of pentylenetetrazol (PTZ) to attenuate $GABA_A$ receptor activity, or the ampakine drug CX546 to potentiate α-amino-3-hydroxy-5-methyl-4-isoxazolepropionic acid (AMPA) glutamate receptor function during emergence from anaesthesia ameliorates neuronal circuit dysfunction and prevents long-term learning deficits in mice.

Methods

Experimental animals

Transgenic mice expressing GCaMP6 slow (GCaMP6s) in layer (L) 2/3 and L5 pyramidal neurones, *Thy*1-GCaMP6s founder line 3, were gifts from Wen-Biao Gan at New York University School of Medicine (New York, NY, USA).[28] Adeno-associated virus (AAV) experiments were conducted with C57BL/6 (stock no. 000664), SST-IRES-Cre (stock no. 013044), PV-IRES-Cre (stock no. 008069), and VIP-IRES-Cre mice (stock no. 010908) purchased from the Jackson Laboratory (Bar Harbor, ME, USA). The mice were group-housed in temperature-controlled rooms on a 12 h light–dark cycle in the Columbia University Eye Institute animal facility (New York, NY, USA). Male animals were randomly assigned to different treatment groups. All animal experiments were carried out in accordance with institutional guidelines and were approved by the Institutional Animal Care and Use Committee at Columbia University Medical Center as consistent with the National Institutes of Health (NIH) Guide for the Care and Use of Laboratory Animals.

Drug injection

For early postnatal anaesthesia, mice were injected i.p. with a single dose of propofol (200 mg kg^{-1}) on Postnatal day 7 (P7), or one dose every other day (P7, P9, and P11) for a total of three doses. Control animals received Intralipid® (Sigma, St. Louis, MO, USA) vehicle injection(s). Consistent with previous studies,[29,30] we found that propofol 200 mg kg^{-1} i.p. induced a surgical plane of anaesthesia and provided immobilisation in P7 mice for ~1 h. During anaesthesia, a heating pad was used to maintain the body temperature of the animal at ~37°C. In a separate group of animals, we measured arterial blood gases under spontaneous respiration (i-STAT System; Abbott Point of Care, Princeton, NJ, USA), which showed normal values of pH and partial pressures of O_2 and CO_2 under this anaesthesia protocol (Supplementary Fig. S1). Pentylenetetrazol (PTZ) (4 mg kg^{-1}) and CX546 (20 mg kg^{-1}) were injected i.p. either alone or at 1 h after propofol administration.

Surgical preparation for imaging awake, head-restrained mice

In vivo Ca^{2+} imaging was performed in awake, head-restrained mice. The surgical procedure for preparing awake animal imaging has been described.[31] In brief, a head holder composed of two metal bars was attached to the skull of the animal to reduce motion-induced artifact. First, surgical anaesthesia was achieved with ketamine 100 mg kg^{-1} and xylazine 15 mg kg^{-1} i.p. (Covetrus, Portland, ME, USA). A midline incision of the scalp exposed the periosteum; the skull region located over the primary motor cortex was identified based on stereotactic coordinates (0.5 mm anterior from the bregma and 1.2 mm lateral from the midline) and marked. A thin layer of glue (LOCTITE® 495, R.S. Hughes Co., Sunnyvale, CA, USA) was first applied to the

entire skull surface and metal bars, and the head holder was then further fortified with dental acrylic cement, leaving the marked skull region exposed between the two bars. After the dental cement was completely dry, a cranial window was created over the marked region. The procedures for preparing a thinned-skull cranial window for two-photon imaging have been described in detail.[32] For open-skull preparation, a small circular craniotomy (1.0–1.5 mm diameter) was made and covered with a round glass coverslip the size of the bone removed. The coverslip was glued to the skull to reduce motion of the exposed brain. Before imaging, mice were given 1 day to recover from the surgery-related anaesthesia and habituated for a few times (10 min each time) to minimise potential stress effects of head restraining and imaging.

In vivo two-photon Ca^{2+} imaging

The genetically encoded Ca^{2+} indicator GCaMP6s was used for Ca^{2+} imaging of pyramidal neurones and interneurones in the motor cortex. We utilised *Thy1*-GCaMP6s mice for imaging pyramidal neurones, and SST, PV, and VIP-Cre lines for interneurone imaging. In *Thy1*-GCaMP6s mice, GCaMP expression in the cortex was sufficient for Ca^{2+} imaging as early as 2 weeks of age. For Cre mice, Cre-dependent GCaMP6s was expressed with recombinant AAV (AAV-CAG-Flex-GCaMP6s or AAV-syn-Flex-GCaMP6s; serotype 2/1; $>2 \times 10^{13}$ [genome copies ml^{-1}] titre; Addgene, Watertown, MA, USA). We injected AAV 0.2 μl (Picospritzer® III; Parker Hannifin Co., Holis, NH, USA; 15 psi; 10 ms; 0.5 Hz) over 10–15 min into L2/3 of the motor cortex using a glass microelectrode around the coordinates of anterior–posterior +0.5 mm (to Bregma), medial–lateral 1.2 mm, and dorsal–ventral 0.3 mm. Mice were injected with AAV at 3–4 months of age and imaged 2 weeks later.

In vivo two-photon Ca^{2+} imaging was performed with a Scientifica (Uckfield, East Sussex, UK) two-photon system equipped with a Ti:sapphire laser (Vision S; Coherent, Santa Clara, CA, USA) tuned to 920 nm. Imaging was performed at 200–350 and 500–700 μm below the pial surface for detecting somata of L2/3 and L5 neurones, respectively, and 20–70 μm for detecting pyramidal neurone dendrites in L1. Time-lapse imaging was performed at one focal plane for pyramidal neurones and at one to three focal planes for interneurones. All experiments were performed using a 25× objective (1.05 numerical aperture) immersed in artificial CSF, and with a 1× (somata) or 3× (dendrites) digital zoom. Images were acquired at a frame rate of 1.69 Hz (2 μs pixel dwell time) at a resolution of 512 × 512 pixels. Duration of imaging and number of repetitions were kept to a minimum to avoid phototoxicity. Image acquisition was performed using ScanImage software (Vidrio Technologies, Ashburn, VA, USA) and analysed *post hoc* using NIH ImageJ as described.[33] Regions of interest (ROI) corresponding to visually identifiable somata or dendritic segments were selected for quantification. The fluorescence time course of each soma or dendritic segment was measured by averaging all pixels within the ROI. The baseline fluorescence signal (F_0) was estimated by detecting inactive portions of the fluorescence time course using an iterative procedure,[34] and $\Delta F/F_0$ was calculated as $(F-F_0)/F_0 \times 100\%$. Ca^{2+} transients were defined as events when changes of fluorescence ($\Delta F/F_0$) observed in ROI were more than one standard deviation (SD) of fluorescence signal at quiet resting states and lasting longer than 0.9 s during the 1 min recording session. The open source tool CaImAn[35] (Python version, released on https://github.com/) was used to correct the motion of raw Ca^{2+} image series using the NoRMCorre algorithm[36] and to temporally deconvolute the $\Delta F/F_0$ signals to extract Ca^{2+} spikes based on the improved fast non-negative deconvolution method.[37,38]

Treadmill training

A treadmill task was used to provide a motor learning experience and to allow two-photon Ca^{2+} imaging and motor learning at the same time. A custom-built treadmill (46 × 15 × 10 cm) was used that allowed head-fixed mice to move their limbs freely to perform running tasks. After the onset of a trial, the belt speed gradually increased from 0 to 8 cm s^{-1} within ~3 s and maintained at 8 cm s^{-1} for the rest of the trial. To obtain footprints, mouse paws were coated with ink and a sheet of white paper was placed on top of the belt during treadmill training. Gait pattern analysis was performed manually offline. Gait pattern was classified as drag, wobble, sweep, and steady run. The mice displayed large proportions of untrained gait features (i.e. drag, wobble, and sweep) when they first ran on the treadmill, whereas the percentage of trained gait feature (i.e. steady run) increased after training. Treadmill performance improvement was presented as the difference in percentage of time spent in steady run (averaged over five trials) between the pre- and post-training sessions.

Novel object recognition test

In all behavioural experiments, researchers were blinded to the experimental condition. Mice were tested for novel object recognition (NOR) in an opaque box (40 × 40 × 35 cm). Behaviour was videotaped and images were analysed with ANY-maze behaviour tracking software (Stoelting; Wood Dale, IL, USA). The mice were handled by the same researcher for 3 days, and then habituated to the testing environment for 30 min with no objects in the chamber. The next day, the mice were placed into the testing environment with two identical sample objects (familiar object) placed in neighbouring corners for 10 min. The mice were removed and returned to their home cages. Then, 6 and 24 h later, the mice were returned to the testing environment for 5 min where one of the sample objects was replaced by a novel object, which differed from the familiar object in shape and texture. Measures of interaction were taken of the amount of time the animal spent with its head and nose oriented towards and within 2 cm of the object. Other types of interactions, such as the animal accidentally touching, sitting, or standing on the object, were not considered exploratory activities. Discrimination index was calculated as the time spent interacting with the novel object divided by the total time spent exploring both objects.

Social preference test

Three-chamber social test was conducted in a Ugo Basile sociability apparatus (Gemonio, VA, Italy) using ANY-Maze software.[39] Each chamber was 20 × 40 × 22 cm, and the dividing walls had small rectangular doors (5 × 8 cm) allowing communication between chambers. The test mouse was first placed in the middle chamber and allowed to explore all three chambers for 10 min. After this habituation period, a familiar mouse from the home cage of the test mouse (cage mate) was randomly placed in a cylinder-shaped wire cage (7 cm in diameter and 15 cm high) in one of the side chambers. A novel, unfamiliar mouse (stranger) was placed in an identical cylinder-shaped wire cage in the other side chamber. The

familiar and unfamiliar mice were of the same sex as the test mouse and had been previously habituated to the wire cage. Both doors to the side chambers were then unblocked, and the test mouse was allowed to explore the entire apparatus in a 10 min session. The test mouse had a choice between the familiar and the unfamiliar mouse. Measures were taken of the amount of time spent in each chamber. Preference index for social novelty was calculated as the time that the test mouse spent in the chamber with the novel, unfamiliar mouse divided by the time spent in the chamber with the familiar mouse.

Open field test

Mice were tested for locomotor functions and anxiety-like behaviours in an opaque box (40 × 40 × 35 cm). The mice were handled by the same researcher for 3 days, and then habituated to the testing environment for 30 min. The next day, the mice were placed into the testing environment for 10 min. Behaviour was videotaped and images were analysed with ANY-maze software. Measures of average speed, maximum speed, and body rotations were used to assess locomotor functions. Anxiety-like behaviours were assessed by the number of entries into the inner zone and the ratio of time that the animal spent in the inner zone relative to the outer zone. The inner zone was defined as a 20 × 20 cm region in the centre of the testing field.

Elevated plus maze test

An elevated plus maze with two open and two enclosed arms of identical dimensions (30 × 10 cm) was used to test anxiety-

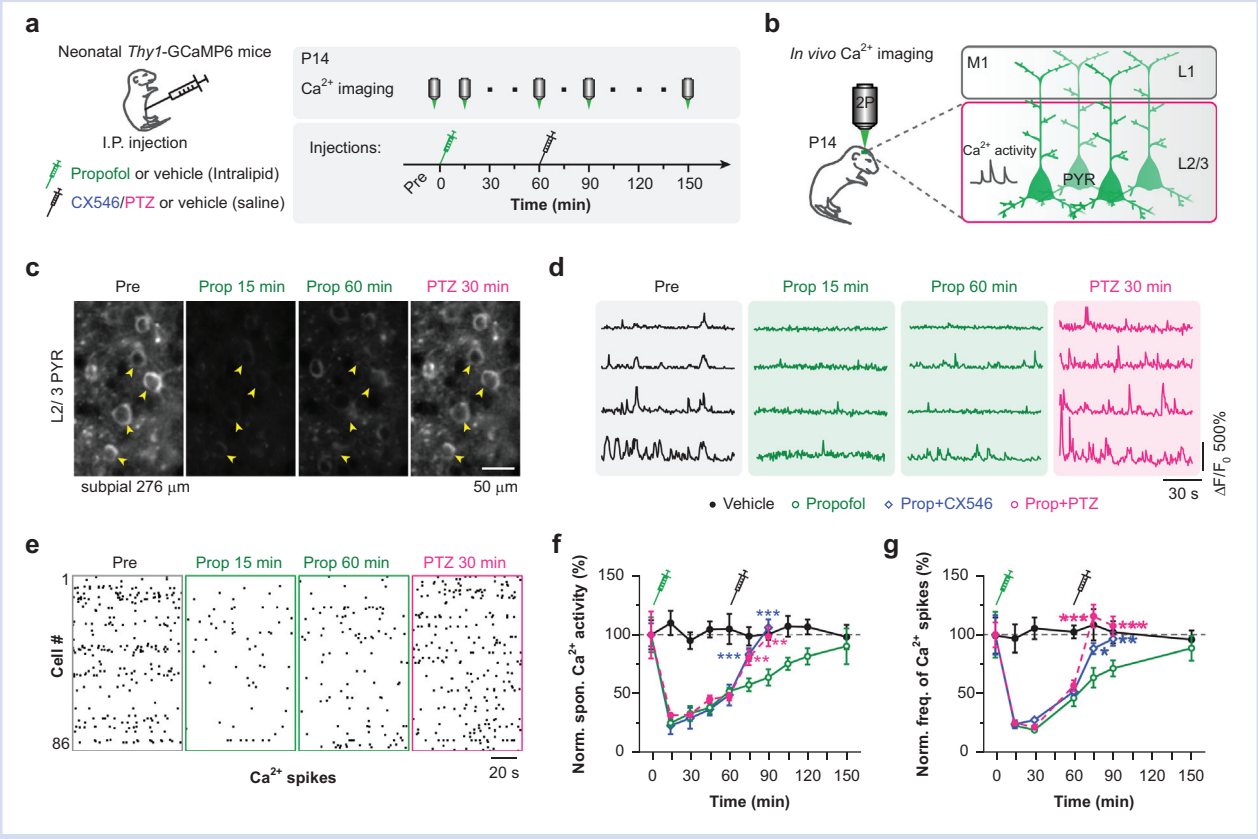

Fig 1. Propofol-induced decrease in neuronal activity persists into anaesthesia recovery period in neonatal mice. (a) Experimental design. (b) Schematic of *in vivo* two-photon Ca^{2+} imaging of L2/3 pyramidal neurones in awake mice at 2 weeks of age. (c) Images of pyramidal (PYR) neurones expressing GCaMP6s before injection (awake), 15 and 60 min after propofol (200 mg kg^{-1} i.p.) injection, and 30 min after PTZ injection (i.e. 90 min after propofol). (d) Ca^{2+} fluorescence traces of representative neurones before and after propofol and PTZ injection. (e) Deconvoluted somatic Ca^{2+} spikes from 86 representative pyramidal cells. (f) Normalised neuronal Ca^{2+} activity over time after propofol and PTZ or CX546 injection (n=225–341 cells from four mice per group); 15 min after PTZ: 80.8 (6.6), t=2.71, P=0.007 *vs* propofol at 75 min: 57.7 (5.4); 30 min after PTZ, 98.7 (8.4), t=3.21, P=0.001 *vs* propofol at 90 min: 63.9 (6.9); 15 min after CX546, 83.3 (5.4), t=3.36, P<0.001 *vs* propofol at 75 min; 30 min after CX546: 106.2 (7.0), t=4.31, P<0.001 *vs* propofol at 90 min. There were no significant changes in neuronal Ca^{2+} activity after Intralipid vehicle injections at 0 min (n=312 cells from four mice). Saline injection at 60 min had no effect on Ca^{2+} activity in propofol-treated mice. (g) Normalised frequency of somatic Ca^{2+} spikes over time after propofol and PTZ or CX546 injection; 15 min after PTZ: 115.8 (9.6), t=4.08, P<0.001 *vs* propofol at 75 min: 63.8 (8.4); 30 min after PTZ, 107.6 (8.2), t=3.36, P<0.001 *vs* propofol at 90 min: 71.7 (6.9); 15 min after CX546, 88.4 (4.6), t=2.58, P=0.010 *vs* propofol at 75 min; 30 min after CX546: 96.6 (5.8), t=2.76, P=0.006 *vs* propofol at 90 min. No significant changes in frequency were found after Intralipid (vehicle of propofol, at 0 min) or saline (vehicle of CX546 or PTZ, at 60 min) injections. Data are presented as mean (standard error of the mean). *P<0.05; **P<0.01; ***P<0.001. Unpaired two-tailed t-test with Welch's correction in (f) and (g). PTZ, pentylenetetrazol.

like behaviour. The joint zone of open and enclosed arms was 10 × 10 cm. The plus maze was elevated 1 m from the floor. Mice were handled by the same researcher for 3 days, and then habituated to the testing environment for 30 min. The next day, the mice were placed into the elevated plus maze for 10 min. Exploratory behaviour was videotaped and analysed with ANY-maze software. Anxiety-like behaviour was assessed by the ratio of time that the animal spent in the open arms relative to the enclosed arms.

Marble burying test

Marble burying test was conducted in a standard cage (29 × 18 × 12 cm) filled with 4 cm depth of corncob bedding with 24 marbles (1.3 cm in diameter) evenly spaced. Mice were handled by the same researcher for 3 days, and then habituated to the testing environment for 30 min. The next day, the mice were placed in the testing cage for 20 min, and then the number of marbles buried was counted. A marble was considered buried if two-thirds of the marble was covered with bedding. Obsessive/compulsive-like behaviour was assessed by the percentage of marbles buried.

Immunohistochemistry and confocal imaging

Mice were deeply anaesthetised and perfused with a phosphate-buffered solution (PBS) and paraformaldehyde (PFA) 4%. The brain was removed and post-fixed in PFA 4% for 3 days and rinsed three times with PBS embedded in agarose 1.5%, and then immersed in PBS. The brain (from +0.3 to +0.7 mm anterior to bregma) was sectioned with a Leica (Buffalo Grove, IL, USA) vibratome (VT1000 S) at 50 and 20 μm thicknesses for soma and synapse immunohistochemistry, respectively. Sections were post-fixed in PFA 4% for 1 h and washed three times with PBS. Floating sections were permeabilised and blocked at room temperature in Triton X-100 0.1% (for soma immunohistochemistry) or saponin 0.1% (for synapse immunohistochemistry) with goat serum 5% in PBS for 1.5 h, and then incubated overnight at 4°C with primary antibodies: mouse anti-NeuN (Millipore [St. Louis, MO, USA]; MAB377; 1:500), rabbit anti-green fluorescent protein (GFP) (Abcam [Cambridge, MA, USA]; ab6556; 1:1500), rabbit anti-VGLUT1 (Sigma [St. Louis, MO, USA]; ABN1647; 1:400), and mouse anti-pan-AMPA receptor (AMPAR) (Sigma; MABN832; 1:300). The sections were then washed three times with PBS and incubated for 2 h at room temperature with secondary antibodies: goat anti-rabbit Alexa Fluor® 488 (Invitrogen [Waltham, MA, USA]; 1:500), goat anti-mouse CF® 543 (Biotium [Fremont, CA, USA]; 1:500), and NeuroTrace™ 435/455 Blue Fluorescent Nissl Stain (Invitrogen; N21479; 1:300), and then Nissl stained. The sections were washed as before and then mounted (SouthernBiotech [Birmingham, AL, USA] mounting medium; 010001) for confocal imaging.

Confocal imaging was performed with a 20× objective on a Nikon Ti laser scanning confocal system (Melville, NY, USA). Images were taken at 1024 × 1024 pixels with a resolution of 0.622 and 0.031 μm pixel^{-1} for visualising somata and synapses, respectively. The fluorophores of NeuroTrace 435, Alexa Fluor 488, and CF543 were excited by 405, 488, and 561 nm lasers, respectively. A z-stack of images was obtained at 2 and 0.3 μm step size for soma and synapse visualisation, and projected at a maximum intensity to generate the final multichannel images, which were then analysed using NIH ImageJ software. The density of neurones (NeuN$^+$) and GCaMP6s-expressing pyramidal neurones (GCaMP$^+$; GFP immunoreactive) in L2/3 and L5 of the motor cortex was quantified as cell number per 100 μm^2 cortical area. The density of glutamatergic boutons (VGLUT1$^+$) and postsynaptic loci expressing AMPARs (AMPAR$^+$) was quantified as immunoreactive puncta number per 100 μm^2 cortical area. A VGLUT1$^+$ or AMPAR$^+$ punctum fulfilling the criteria of roundness at 0.5–1, mean fluorescent intensity at 3 SD above background, and diameter at 0.2–1.6 μm was counted automatically by the software.

Statistical analysis

Prism software (GraphPad 7.0; San Diego, CA, USA) was used to conduct the statistical analysis. Data were presented as mean (standard error of the mean). Tests for differences between two populations were performed using two-tailed Student's *t*-test or non-parametric Mann–Whitney *U*-test as specified in the figure legend. Tests for differences between multiple populations were performed using non-parametric Kolmogorov–Smirnov testing. No data points were excluded from the statistical analysis, and variance was similar between groups being statistically compared. Significant levels were set at $P \leq 0.05$.

Results

Propofol administration reduces pyramidal neuronal activity in neonatal mice

We used *in vivo* two-photon Ca^{2+} imaging of L2/3 pyramidal neurones in the primary motor cortex of 2-week-old mice throughout anaesthesia and recovery to determine the effect of propofol anaesthesia on neuronal activity (Fig. 1a). Transgenic mice expressing the genetically encoded calcium indicator GCaMP6s specifically in cortical pyramidal neurones were used to monitor neuronal activity[28] (Fig. 1b). The i.p. dose of propofol required to induce a surgical plane of anaesthesia in young mice is 200 mg kg^{-1}.[29,30] We found that the level of somatic Ca^{2+} transients in cortical neurones was greatly reduced at 15 min after propofol 200 mg kg^{-1} i.p. compared with pre-injection baseline (i.e. resting awake) ($\Delta F_{Propofol}/\Delta F_{wake}$: 25.4% [3.1%]; $P<0.001$) (Fig. 1c–g). Mice started to show voluntary movements around 1 h after propofol injection, but the level of somatic Ca^{2+} transients remained ~50% lower than the awake state ($\Delta F_{Propofol}/\Delta F_{wake}$: 52.2% [3.0%]; $P<0.001$). The reduction in somatic Ca^{2+} transients persisted for at least 2 h after propofol injection ($\Delta F_{Propofol}/\Delta F_{wake}$: 81.8% [6.9%]; $P=0.012$), indicating a prolonged reduction of neuronal firing rate that persists into the anaesthesia recovery period.

Given that propofol activates $GABA_A$ receptor,[40] we reasoned that suppression of $GABA_A$ receptor signalling during anaesthesia recovery might be effective in restoring neuronal activity in propofol-treated mice. To test this, we treated mice with PTZ (4 mg kg^{-1}, a non-convulsant dose[41]), a non-competitive $GABA_A$ receptor antagonist with a history of medical use,[42] 1 h after propofol injection (Fig. 1a). Neuronal activity was significantly increased within 15 min after PTZ injection and 30 min after PTZ injection (i.e. 90 min after propofol injection) somatic Ca^{2+} transients in cortical pyramidal neurones were comparable with those during the pre-anaesthesia awake state (Fig. 1c–g). Thus, suppression of $GABA_A$ receptor function was effective in restoring neuronal activity after propofol anaesthesia.

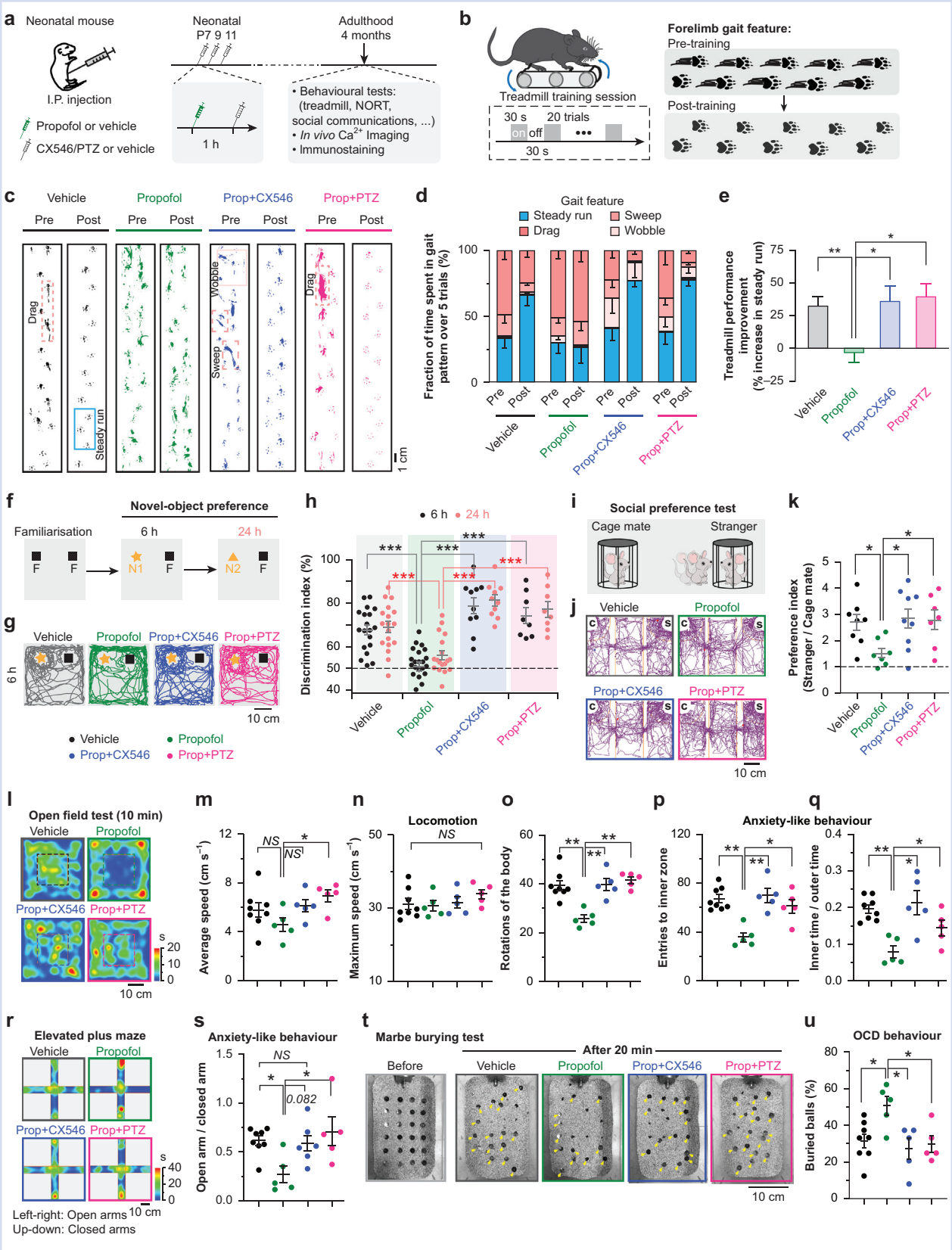

Fig 2. Repeated neonatal propofol anaesthesia causes behavioural impairments that are rescued by PTZ or CX546 treatment. (a) Experimental design. (b) Schematic of treadmill training. (c) Representative gait patterns of mice running on a treadmill before and after training.

In addition to PTZ, administration of an ampakine drug, CX546, to potentiate AMPARs was also effective in restoring activity during emergence from propofol anaesthesia. Two-week-old mice were treated with CX546 20 mg kg^{-1} i.p. 1 h after propofol injection (Fig. 1a), and neuronal activity was significantly increased within 15 min after CX546 injection (Fig. 1f and g). At 30 min after CX546 injection, somatic Ca^{2+} transients in cortical pyramidal neurones were comparable with those during the pre-anaesthesia awake state (Fig. 1f and g), indicating that potentiation of AMPAR function was also effective in restoring neuronal activity after anaesthesia. Administration of PTZ 4 mg kg^{-1} or CX546 20 mg kg^{-1} alone in non-anaesthetised mice transiently and moderately increased Ca^{2+} activity in cortical pyramidal neurones (Supplementary Fig. S2). Together, these results show that attenuation of $GABA_A$ receptor activity or potentiation of AMPAR activity helps to restore neuronal activity during emergence from propofol anaesthesia.

Repeated propofol exposure causes behavioural impairments in adult mice

To investigate whether exposure to propofol during early postnatal development causes behavioural impairments in later life, we treated mice with one or three doses of propofol (200 mg kg^{-1}) at P7–P11, which represent the period of rapid synaptogenesis. Control mice received Intralipid vehicle injections (Fig. 2a and Supplementary Fig. S3a). Four months later, all groups had normal body weight (Supplementary Fig. S4) and were trained to run on a treadmill where they learned to change their gait patterns progressively (Fig. 2b).[43] The mice displayed large proportions of drag, wobble, and sweep when they first ran on the treadmill, whereas the percentage of steady run increased with training (Fig. 2c). We observed significant increases in steady run in vehicle-treated control mice after 20-trial training. A single dose of propofol had no apparent effect on treadmill performance (Supplementary Fig. S3a–c), but mice subjected to three doses of propofol showed little training-related performance improvement (Fig. 2c–e). This deficit in motor skill learning was not observed in mice that received PTZ (4 mg kg^{-1}) or CX546 (20 mg kg^{-1}) 1 h after each propofol injection (Fig. 2c–e). Administration of PTZ or CX546 alone had no significant effects on treadmill performance in adulthood (Supplementary Fig. S3a–c). Thus, repeated propofol exposure during early brain development resulted in motor learning impairments in adulthood.

In addition to motor learning, we also examined the cognitive, social, and emotional aspects of behaviour in adult mice that had been administered vehicle, one or three doses of propofol, propofol plus CX546, or propofol plus PTZ during P7–P11. In the NOR test, preference to explore the novel object reflects recognition memory. We separated the training and the test sessions by 6 and 24 h to examine short- and long-term memory, respectively (Fig. 2f). Whilst vehicle-treated controls showed a preference towards the novel object, mice treated with three but not one dose of propofol showed no such preference at either 6 or 24 h after training (Fig. 2g and h and Supplementary Fig. S3d). This deficit in NOR memory was not observed in mice administered PTZ or CX546 after propofol (Fig. 2g and h).

Tests for social memory were performed in a three-chamber social apparatus where control mice spent more time exploring the stranger mouse than their cage mate (Fig. 2i). The propofol-exposed mice spent similar amounts of time with familiar and unfamiliar mice, which contrasted with control and propofol plus PTZ or CX546 mice that preferentially interacted with unfamiliar mice (Fig. 2j and k). Additionally, we found that repeated propofol exposure caused anxiety-like behaviour in adult mice, as evidenced in open field and elevated plus maze tests, and obsessive/compulsive-disorder-like behaviour, as displayed in the marble burying

(d) Measures of various gait features before and after training (n=4–8 mice per group). Steady, wobble, sweep, and drag of vehicle pre: 29.0 (6.7), 1.1 (0.8), 17.6 (6.9), 52.3 (7.5); post: 60.6 (7.2), 2.2 (1.3), 8.0 (2.0), 29.3 (6.4); propofol pre: 26.7 (6.8), 5.3 (3.8), 14.1 (4.0), 53.9 (6.9); post: 23.9 (10.7), 0.8 (0.8), 19.2 (7.0), 56.2 (9.6); propofol+CX546 pre: 38.5 (8.6), 23.1 (11.2), 14.8 (5.8), 23.6 (6.2); post: 65.3 (3.8), 19.6 (16.7), 2.5 (0.7), 12.6 (5.4); propofol+PTZ pre: 30.3 (7.5), 12.6 (8.2), 15.8 (6.0), 41.3 (12.4); post: 62.5 (4.1), 15.4 (8.1), 5.8 (3.2), 16.3 (4.2). (e) Treadmill performance improvement. Vehicle: 32.2 (7.0); propofol: −3.3 (7.4), P=0.008 *vs* vehicle; propofol+CX546: 35.8 (11.8), P=0.71 *vs* vehicle, P=0.042 *vs* propofol; propofol+PTZ: 39.6 (9.6), P=0.42 *vs* vehicle, P=0.010 *vs* propofol. (f) Schematic and timeline for novel object recognition (NOR) test. (g) Representative trajectories of mice in NOR test. (h) Discrimination ratio in NOR test (n=8–23 mice per group). 6 h, vehicle: 67.8 (2.2), propofol: 50.9 (1.8), P<0.001 *vs* vehicle; propofol+CX546: 79.0 (3.7), P=0.022 *vs* vehicle, P<0.001 *vs* propofol; propofol+PTZ: 74.3 (3.7), P=0.26 *vs* vehicle, P<0.001 *vs* propofol. 24 h, vehicle: 69.1 (2.5), propofol: 56.1 (2.0), P<0.001 *vs* vehicle; propofol+CX546: 81.4 (2.6), P=0.0072 *vs* vehicle, P<0.001 *vs* propofol; propofol+PTZ: 77.2 (3.6), P=0.080 *vs* vehicle, P=0.001 *vs* propofol. (i) Schematic of social preference test. (j) Representative trajectories in the social test. (k) Social preference index (n=7–9 mice per group). Vehicle: 2.7 (0.3), propofol: 1.5 (0.2), P=0.021 *vs* vehicle; propofol+CX546: 2.8 (0.4), P=0.96 *vs* vehicle; propofol+PTZ: 2.8 (0.4), P=0.87 *vs* vehicle. (l) Representative heat map of trajectories in the open field test. Dashed line indicates the border of inner and outer zones. (m–o) Locomotor parameters measured in the open field test (n=5–8 mice). Average speed (cm s^{-1}), vehicle: 5.8 (0.6); propofol: 4.6 (0.6), P=0.17 *vs* vehicle; propofol+CX546: 6.1 (0.5), P=0.15 *vs* propofol; propofol+PTZ: 6.9 (0.5), P=0.016 *vs* propofol; maximum speed (cm s^{-1}), vehicle: 31.2 (1.5); propofol: 30.8 (1.4), P=0.99 *vs* vehicle; propofol+CX546: 31.7 (1.5), P=0.69 *vs* propofol; propofol+PTZ: 33.9 (1.3), P=0.15 *vs* propofol; rotations of the body, vehicle: 39.4 (2.0); propofol: 25.8 (1.5), P=0.002 *vs* vehicle; propofol+CX546: 39.8 (2.4), P=0.008 *vs* propofol; propofol+PTZ: 41.6 (1.4), P=0.008 *vs* propofol. (p–q) Anxiety-like behaviours measured in the open field test (n=5–8 mice). Entries to inner zone, vehicle: 67.1 (3.3); propofol: 35.80 (3.81), P=0.002 *vs* vehicle; propofol+CX546: 70.00 (5.71), P=0.008 *vs* propofol; propofol+PTZ: 61.20 (5.7), P=0.002 *vs* propofol; ratio of inner *vs* outer zone, vehicle: 0.20 (0.01); propofol: 0.08 (0.02), P=0.002 *vs* vehicle; propofol+CX546: 0.21 (0.03), P=0.003 *vs* propofol; propofol+PTZ: 0.16 (0.02), P=0.003 *vs* propofol. (r) Representative heat map of mouse trajectories in the elevated plus maze test. Left to right: open arms, up–down: closed arms. (s) Anxiety-like behaviours measured in the elevated plus maze test (n=5–8 mice). Vehicle: 0.62 (0.049); propofol: 0.27 (0.09), P=0.011 *vs* vehicle; propofol+CX546: 0.59 (0.09), P=0.082 *vs* propofol, P=0.49 *vs* vehicle; propofol+PTZ: 0.71 (0.15), P=0.032 *vs* propofol. (t) Representative pictures of marble burying tests. Yellow arrowheads indicate exposed balls. (u) Obsessive/compulsive-disorder (OCD)-like behaviour measured in marble burying tests (n=5–8 mice). Vehicle: 31.8 (3.8); propofol: 50.8 (5.2), P=0.020 *vs* vehicle; propofol+CX546: 27.5 (5.7), P=0.040 *vs* propofol; propofol+PTZ: 30.0 (4.4), P=0.040 *vs* propofol. Data are presented as mean (standard error of the mean). *P<0.05; **P<0.01; ***P<0.001; *NS*, not significant. Two-tailed Mann–Whitney *U*-test in (e), (h), (k), (m–q), (s), and (u). PTZ, pentylenetetrazol.

test (Fig. 2l–u). Mice that received PTZ or CX546 after repeated propofol exposure or a single dose of propofol showed similar performance as control mice in these tests (Fig. 2l–u and Supplementary Fig. S3e–l).

Collectively, these results show that repeated propofol anaesthesia causes persistent cognitive and behavioural deficits in neonatal mice, which can be prevented by pharmacologically potentiating neuronal activity during anaesthesia recovery.

Repeated propofol exposure causes reduced neuronal density in the cortex

To identify cortical changes associated with motor learning impairment caused by neonatal anaesthesia, we first examined the density of neurones in the motor cortex. Transgenic *Thy*1-GCaMP6s mice were administered three doses of propofol during P7–P11 and assessed at 4 months of age. Immunostaining in the motor cortex revealed a 10–18% reduction in the density of NeuN$^+$ cells and GCaMP6$^+$ pyramidal neurones in both L2/3 and L5 of the motor cortex after repeated propofol exposure (Fig. 3a–c and Supplementary Fig. S5). In a separate set of animals, we performed immunostaining of vGLUT1 and AMPARs in the cortex of wild-type mice with or without early propofol exposure (Fig. 3d). Analysis of vGLUT1, a presynaptic marker of glutamatergic synapses, in L1 of the motor cortex showed a ~30% reduction in expression in propofol-treated mice as compared with vehicle-treated controls (Fig. 3e). The number of AMPAR$^+$ puncta in L1 of the motor cortex was also reduced (Fig. 3f). These results indicate that repeated neonatal anaesthesia caused a reduction in glutamatergic neurones and synapses. Mice administered PTZ or CX546 after propofol exhibited a normal number of cortical neurones and vGLUT1$^+$ and AMPAR$^+$ puncta in adulthood (Fig. 3a–f), suggesting that potentiating neuronal activity during the post-anaesthesia period prevented neuronal and synaptic loss after early-life anaesthesia.

Repeated propofol exposure effects on pyramidal neurone activity

The aforementioned results of decrease in synaptic density in the motor cortex after repeated propofol exposure suggest possible functional deficits of cortical neurones. Using *in vivo* two-photon Ca^{2+} imaging in awake, head-restrained mice, we examined the activity of pyramidal neurones in L2/3 (200–350 μm below pial surface) and L5 (500–700 μm below pial surface) of the motor cortex when the mice were quietly resting or running on the treadmill (Fig. 4a). Consistent with previous studies, we found that both L2/3 and L5 pyramidal neurones responded to treadmill running and exhibited a marked increase in somatic Ca^{2+} transients (Fig. 4b). We classified active cells into three populations: cells active only during resting, cells active only during running, and cells active during both resting and running (Fig. 4c and d). Comparing repeated propofol with vehicle-treated mice, we observed 40% and 26% reductions in L2/3 and L5, respectively, in the total number of active cells during 1 min of Ca^{2+} recording (30 s treadmill off followed by 30 s treadmill on) (Fig. 4e). For each population of cells, the average somatic Ca^{2+} activity was significantly lower in repeated propofol- than vehicle-treated mice, under both resting and running states (Fig. 4f–i). Mice administered PTZ or CX546 after propofol showed a comparable number of active cells in both L2/3 and L5 relative to vehicle controls (Fig. 4e). Furthermore, PTZ and CX546 increased somatic Ca^{2+} activity to the level in vehicle-treated controls (Fig. 4f–i). These results indicate that neonatal propofol anaesthesia reduced pyramidal neurone activity in the adult motor cortex, which could be reversed by PTZ and CX546.

Unlike repeated propofol exposure, a single dose of propofol at P7 did not cause changes of pyramidal neurone activity in L2/3 and L5 of the adult motor cortex (Supplementary Fig. S6). Thus, repeated propofol anaesthesia during early postnatal development caused persistent hypofunction of cortical pyramidal neurones, which could be rescued by potentiating neuronal activity during anaesthesia recovery.

Effect of dendritic Ca^{2+} transients in cortical pyramidal neurones

Many lines of evidence indicate that dendritic Ca^{2+} transients are critical for excitatory neurone plasticity and function.[43–45] We imaged and measured Ca^{2+} activity in the apical tuft branches (20–70 μm below pial surface) of L2/3 and L5 pyramidal neurones under both quiet resting and treadmill running conditions (Fig. 5). In line with previous reports,[43] we observed a significant increase in the number of dendritic Ca^{2+} spikes in mice running on the treadmill than in the quiet awake state (Fig. 5a). In both vehicle- and repeated propofol-treated mice, dendritic Ca^{2+} transients detected with GCaMP6s occurred across long stretches of dendrites with comparable $\Delta F/F_0$ and lasted several seconds (Fig. 5b and c). Comparing propofol- with vehicle-treated mice, we found that the average activity of dendritic Ca^{2+} spikes was substantially decreased under both resting and running conditions (running: 113.6% [1.8%] *vs* 138.5% [1.8%]; $P<0.001$) (Fig. 5d and e). Moreover, the average length of dendritic segments showing Ca^{2+} spikes was also reduced in propofol-treated mice as compared with vehicle-treated controls (running: 31.9 [0.7] μm *vs* 41.5 [0.9] μm; $P<0.001$) (Fig. 5f and g). These propofol-induced changes were not observed in mice that were administered PTZ or CX546 after propofol exposure (Fig. 5d–i). Because dendritic Ca^{2+} spikes trigger large Ca^{2+} influx into dendrites, these results suggest a decrease in excitatory inputs onto cortical pyramidal neurones after repeated propofol anaesthesia, consistent with the reduction of vGLUT1 and AMPAR expressions in L1 of the cortex (Fig. 3d–f). Thus, repeated propofol exposure in neonates induced a reduction of pyramidal neurone dendritic activity.

Repeated propofol exposure effects on cortical inhibitory interneurone activity

Recent studies have shown that SST-expressing inhibitory interneurones have an important role in regulating dendritic and somatic activities of pyramidal neurones.[34,43,46,47] To measure the impact of propofol on SST cell responses, we used *in vivo* Ca^{2+} imaging to examine the activity of SST cells expressing GCaMP6s after repeated propofol or vehicle injections at P7, P9, and P11 (Fig. 6a). SST-IRES-Cre mice were injected with Cre-dependent AAV to induce expression of GCaMP6s specifically in SST cells. At 4 months of age, spontaneous activity of SST cells was significantly reduced in propofol-treated mice compared with vehicle-treated controls (Fig. 6b–f). For animals trained on the treadmill, running-evoked SST cell activity was substantially lower in propofol- than vehicle-treated mice (propofol: 121.0% [2.7%]; vehicle: 219.6% [4.3%]; $P<0.001$). These *in vivo* Ca^{2+} recordings show

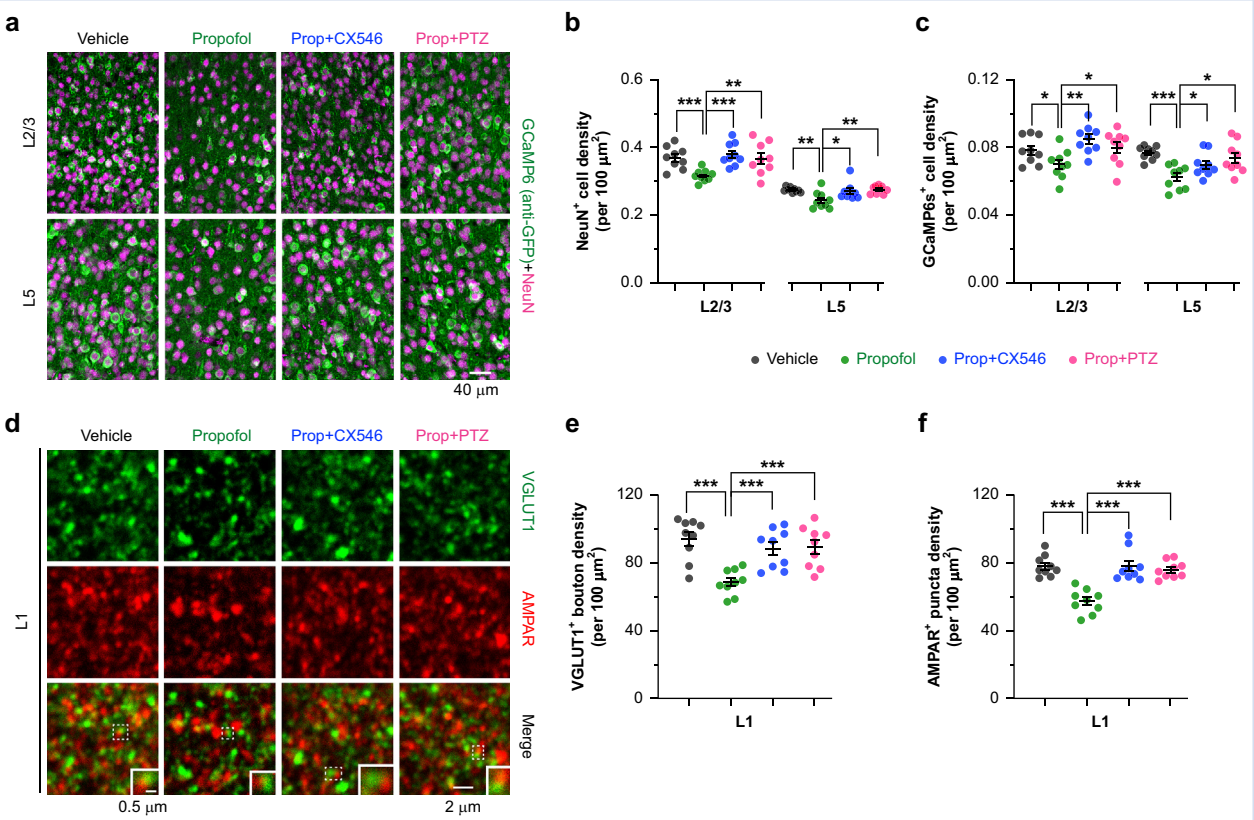

Fig 3. Density of cortical neurones is reduced after repeated neonatal propofol anaesthesia and is rescued by PTZ or CX546 treatment. (a) Representative coronal sections of the mouse motor cortex stained for NeuN (a pan-neuronal marker; magenta) and GCaMP6s (anti-GFP immunoreactive; green) in layers 2/3 and 5. Density of (b) $NeuN^+$ cells and (c) $GCaMP6s^+$ pyramidal neurones in layers 2/3 and 5 (n=9 brain slices from three mice per group; unit: cell number per 100 μm^2). For $NeuN^+$ cells in L2/3 ($\times 10^{-2}$), vehicle: 36.9 (1.1); propofol: 31.4 (0.6), t=4.48, degree of freedom (df)=12.65, P<0.001 *vs* vehicle; propofol+CX546: 37.9 (1.1), t=5.14, df=12.43, P<0.001 *vs* propofol; propofol+PTZ: 36.7 (1.6), t=3.16, df=10.4, P=0.010 *vs* propofol; for $NeuN^+$ cells in L5 ($\times 10^{-2}$), vehicle: 27.4 (0.2); propofol: 24.3 (0.8), t=3.59, df=9.48, P=0.005 *vs* vehicle; propofol+CX546: 27.0 (0.8), t=2.27, df=16.00, P=0.037 *vs* propofol; propofol+PTZ: 27.6 (0.4), t=3.57, df=11.15, P=0.004 *vs* propofol. For $GCaMP6s^+$ cells in L2/3 ($\times 10^{-2}$), vehicle: 7.8 (0.3); propofol: 7.0 (0.3), t=2.14, df=15.98, P=0.048 *vs* vehicle; propofol+CX546: 8.5 (0.3), t=3.80, df=15.99, P=0.002 *vs* propofol; propofol+PTZ: 8.0 (0.3), t=2.25, df=15.51, P=0.039 *vs* propofol; for $GCaMP6s^+$ cells in L5 ($\times 10^{-2}$), vehicle: 7.7 (0.1); propofol: 6.2 (0.2), t=5.26, df=12.41, P<0.001 *vs* vehicle; propofol+CX546: 7.0 (0.2), t=2.17, df=16.00, P=0.046 *vs* propofol; propofol+PTZ: 7.4 (0.3), t=2.93, df=15.14, P=0.010 *vs* propofol. (d) Representative coronal sections of the mouse motor cortex stained for vGLUT1 (green) and AMPAR (red) in layer 1. Insets: pairs of juxtaposed $vGLUT1^+$ bouton and $AMPAR^+$ postsynaptic loci. Density of (e) $vGLUT1^+$ boutons and (f) $AMPAR^+$ puncta in L1 (n=9 brain slices from three mice per group; unit: punctum number per 100 μm^2). $vGLUT1^+$ boutons, vehicle: 94.3 (4.2); propofol: 68.8 (2.5), t=5.27, df=13.13, P=0.001 *vs* vehicle; propofol+CX546: 88.5 (3.8), t=4.30, df=13.74, P<0.001 *vs* propofol; propofol+PTZ: 89.5 (4.0), t=4.36, df=13.36, P<0.001 *vs* propofol. $AMPAR^+$ puncta, vehicle: 78.1 (2.1); propofol: 57.2 (2.4), t=6.66, df=15.72, P<0.001 *vs* vehicle; propofol+CX546: 78.1 (3.1), t=5.31, df=14.86, P<0.001 *vs* propofol; propofol+PTZ: 75.9 (1.7), t=6.46, df=14.39, P<0.001 *vs* propofol. Data are presented as mean (standard error of the mean). *P<0.05; **P<0.01; ***P<0.001. Unpaired two-tailed t-test with Welch's correction in (b), (c), (e), and (f). AMPAR, α-amino-3-hydroxy-5-methyl-4-isoxazolepropionic acid receptor; PTZ, pentylenetetrazol.

that propofol treatment induced a marked and persistent reduction in SST cell activity in the motor cortex.

In addition to SST neurones, we investigated whether PV-positive interneurones were affected by propofol anaesthesia using PV-IRES-Cre mice expressing GCaMP6s. We found that PV cells also displayed a marked reduction in neuronal activity in propofol-treated mice as compared with vehicle-treated controls under both resting and treadmill running states (running: 40.5% [0.9%] *vs* 139.5% [3.7%]; P<0.001) (Fig. 6g–k). Because SST and PV neurones target tuft dendrites and perisomatic regions of pyramidal cells, respectively, reductions of Ca^{2+} activity from these cells suggest a reduced inhibitory control of input and output of excitatory neurones.

Vasoactive intestinal polypeptide-expressing interneurones represent another major inhibitory subclass in the neocortex that directly inhibits the activity of both SST- and PV-expressing interneurones *in vitro* and *in vivo*.[48] To determine whether VIP neurone function might also be altered after neonatal propofol anaesthesia, we infected VIP-IRES-Cre mice with AAV virus encoding GCaMP6s and imaged Ca^{2+} activity of VIP neurones. Similar to what was observed in SST and PV cells, we found a significant decrease in the activity of VIP neurones in propofol- *vs* vehicle-treated mice under quiet

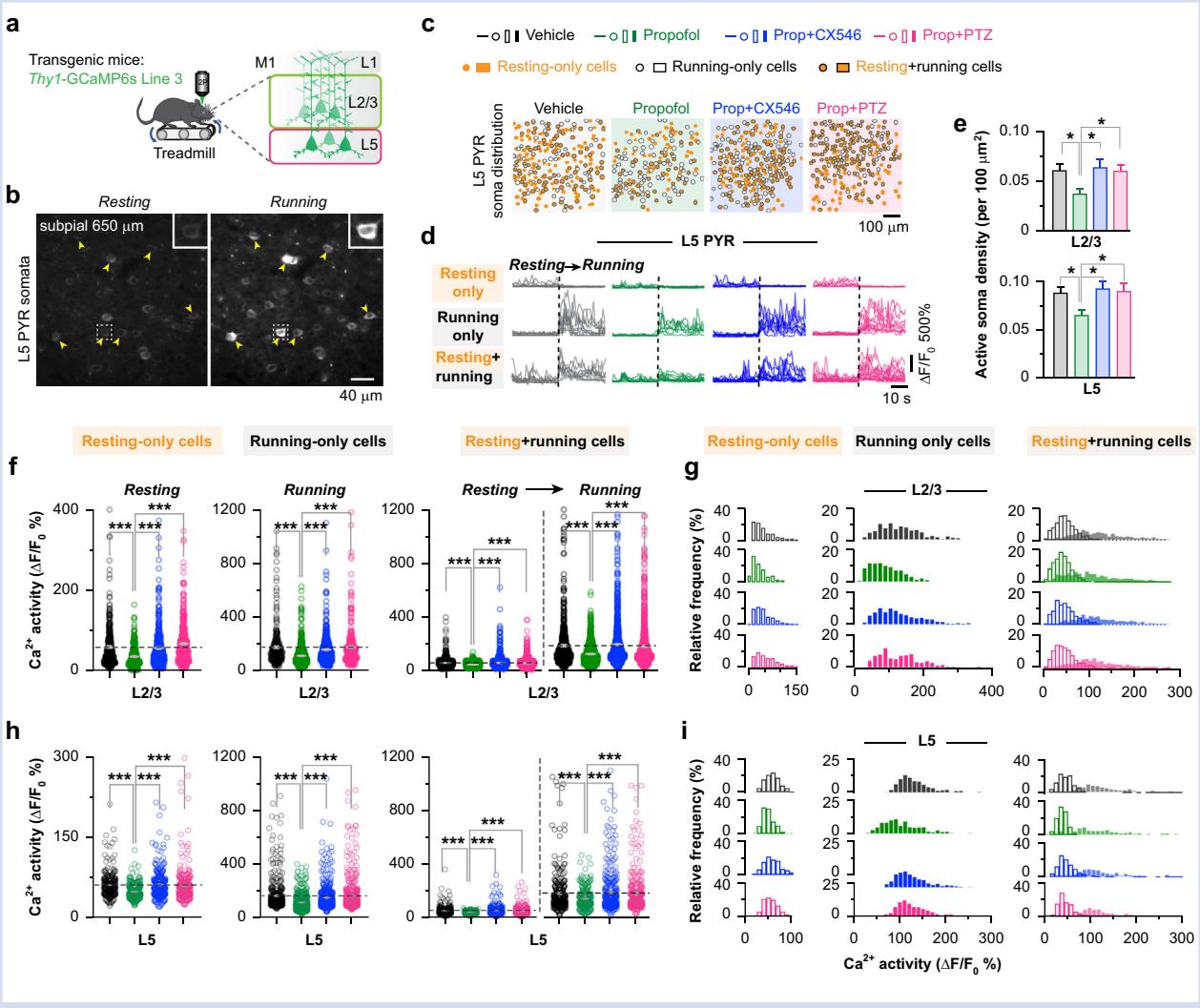

Fig 4. Pyramidal neuronal activity is reduced after repeated neonatal propofol anaesthesia and is rescued by PTZ or CX546 treatment. (a) Schematic of two-photon Ca^{2+} imaging in cortical pyramidal (PYR) neurones during treadmill training. (b) Representative images of L5 somata expressing GCaMP6s during resting and running. (c) Representative maps showing the distribution of L5 somata activated during 1 min Ca^{2+} recording. Filled tangerine dots and empty grey circles represent cells active during resting and running, respectively. (d) Ca^{2+} fluorescence traces of L5 somata during resting and running. Examples of 1 min traces are shown. (e) Density of active neurones in L2/3 and L5 of the motor cortex (cell number per 100 μm^2). For L2/3 ($\times 10^{-2}$), vehicle: 6.0 (0.7); propofol: 3.6 (0.5), P=0.030 *vs* vehicle; propofol+CX546: 6.3 (0.9), P=0.81 *vs* vehicle, P=0.047 *vs* propofol; propofol+PTZ: 5.9 (0.7), P=0.93 *vs* vehicle, P=0.028 *vs* propofol. For L5 ($\times 10^{-2}$), vehicle: 8.7 (0.7); propofol: 6.4 (0.6), P=0.031 *vs* vehicle; propofol+CX546: 9.2 (0.8), P=0.65 *vs* vehicle, P=0.032 *vs* propofol; propofol+PTZ: 8.9 (0.9), P=0.87 *vs* vehicle, P=0.048 *vs* propofol. (f) Measures of average Ca^{2+} activity in L2/3 somata during resting or running (n=998–1174 cells from four to five mice per group). For resting-only cells, vehicle: 62.1 (1.3); propofol: 49.8 (0.9), P<0.001 *vs* vehicle; propofol+CX546: 62.8 (1.6), P=0.66 *vs* vehicle, P<0.001 *vs* propofol; propofol+PTZ: 61.3 (1.9), P=0.059 *vs* vehicle, P<0.001 *vs* propofol. For running-only cells, vehicle: 162.5 (4.9); propofol: 112.2 (2.7), P<0.001 *vs* vehicle; propofol+CX546: 148.5 (4.5), P=0.13 *vs* vehicle, P<0.001 *vs* propofol; propofol+PTZ: 162.1 (5.2), P=0.25 *vs* vehicle, P<0.001 *vs* propofol. For resting+running cells during resting state, vehicle: 55.4 (1.6); propofol: 42.4 (0.73), P<0.001 *vs* vehicle; propofol+CX546: 55.4 (1.8), P=0.33 *vs* vehicle, P<0.001 *vs* propofol; propofol+PTZ: 52.6 (1.53), P=0.052 *vs* vehicle, P<0.001 *vs* propofol; during running state, vehicle: 186.9 (10.2); propofol: 145.5 (5.0), P<0.001 *vs* vehicle; propofol+CX546: 195.2 (9.7), P=0.60 *vs* vehicle, P=0.049 *vs* propofol; propofol+PTZ: 187.7 (9.5), P=0.61 *vs* vehicle, P=0.022 *vs* propofol. (g) Distribution of Ca^{2+} activity in individual somata of L2/3 during resting or running. (h) Measures of average Ca^{2+} activity in L5 somata during resting or running (n=1347–1992 cells from four to five mice per group). For resting-only cells, vehicle: 58.4 (3.2); propofol: 35.5 (1.8), P<0.001 *vs* vehicle; propofol+CX546: 56.8 (2.7), P=0.66 *vs* vehicle, P<0.001 *vs* propofol; propofol+PTZ: 67.8 (2.8), P=0.051 *vs* vehicle, P<0.001 *vs* propofol. For running-only cells, vehicle: 171.5 (9.2); propofol: 107.4 (2.9), P<0.001 *vs* vehicle; propofol+CX546: 154.1 (6.3), P=0.13 *vs* vehicle, P<0.001 *vs* propofol; propofol+PTZ: 172.6 (8.8), P=0.89 *vs* vehicle, P<0.001 *vs* propofol. For resting+running cells during resting state, vehicle: 55.5 (1.4); propofol: 43.2 (0.7), P<0.001 *vs* vehicle; propofol+CX546: 56.1 (1.3), P=0.11 *vs* vehicle, P<0.001 *vs* propofol; propofol+PTZ: 53.3 (1.1), P=0.071 *vs* vehicle, P<0.001 *vs* propofol; during running state, vehicle: 184.3 (7.8); propofol: 122.4 (3.2), P<0.001 *vs* vehicle; propofol+CX546: 192.1 (5.9), P=0.43 *vs* vehicle, P<0.001 *vs* propofol; propofol+PTZ: 180.5 (5.6), P=0.47 *vs* vehicle, P<0.001 *vs* propofol. (i) Distribution of Ca^{2+} activity in individual somata of L5 during resting or running. Data are presented as mean (standard error of the mean). *P<0.05; ***P<0.001. (e) Two-tailed Mann–Whitney U-test and (f) and (h) Kolmogorov–Smirnov's test. PTZ, pentylenetetrazol.

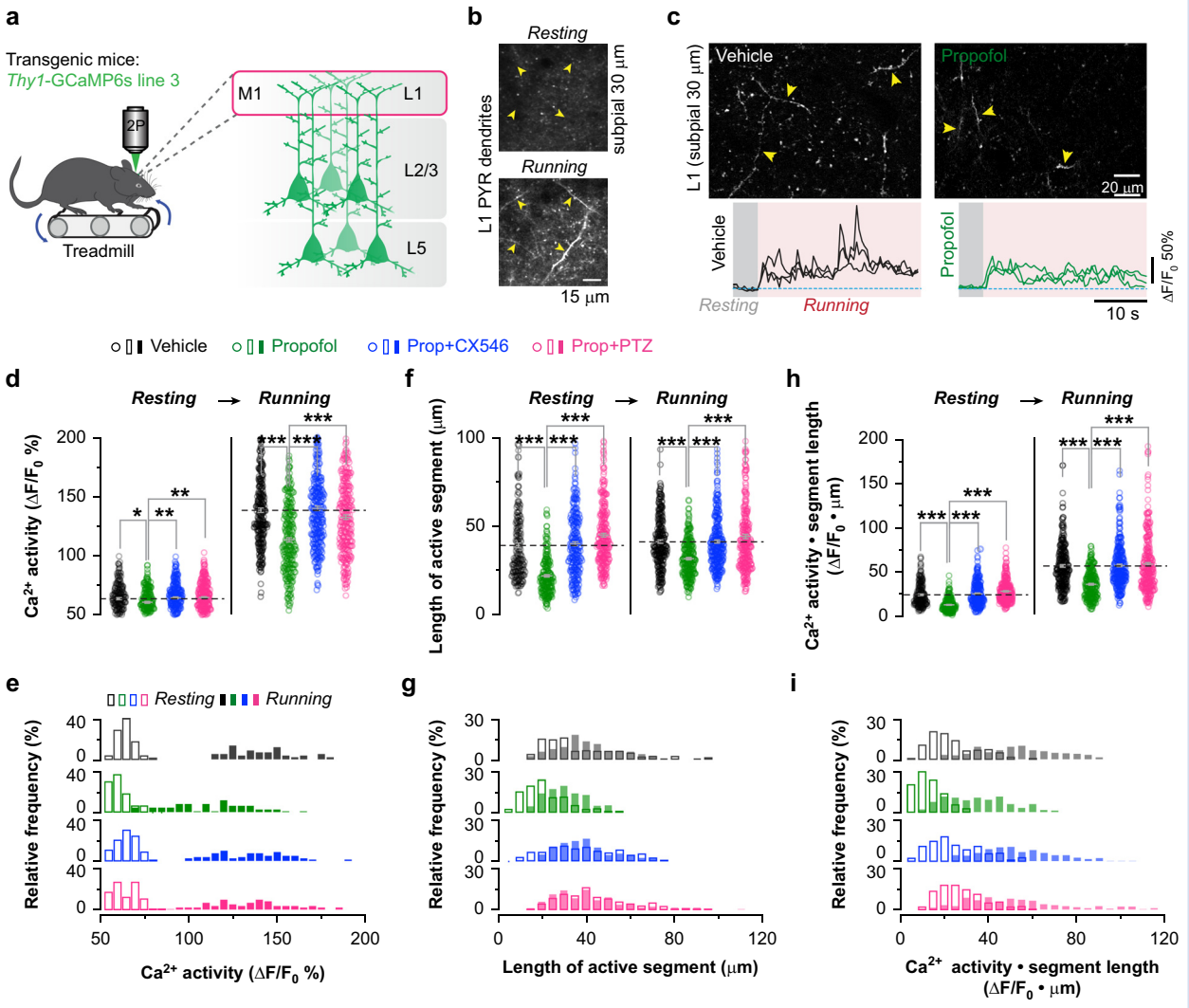

Fig 5. Dendritic activity is reduced after repeated neonatal propofol anaesthesia and rescued by PTZ or CX546 treatment. (a) Schematic of Ca^{2+} imaging in L1 of the motor cortex during treadmill training. (b) Images of tuft dendrites expressing GCaMP6s during resting and running. Running-induced Ca^{2+} transients were visible over long dendritic segments (yellow arrowheads). (c) Representative images and calcium fluorescence traces of dendrites in vehicle- and propofol-treated mice. (d), (f), and (h) Measures of average dendritic Ca^{2+} activity and length of active dendritic segments during resting and running (n=213–296 dendritic segments from three to five mice per group). For dendritic Ca^{2+} activity during resting state, vehicle: 63.9 (0.8); propofol: 60.9 (0.8), P=0.038 *vs* vehicle; propofol+CX546: 64.7 (0.8), P=0.67 *vs* vehicle, P=0.002 *vs* propofol; propofol+PTZ: 64.9 (0.8), P=0.48 *vs* vehicle, P=0.004 *vs* propofol; during running state, vehicle: 138.5 (1.8); propofol: 113.6 (1.8), P<0.001 *vs* vehicle; propofol+CX546: 140.0 (1.9), P=0.84 *vs* vehicle, P<0.001 *vs* propofol; propofol+PTZ: 132.6 (1.9), P=0.10 *vs* vehicle, P<0.001 *vs* propofol. For length of active dendritic segments during resting state, vehicle: 39.3 (1.3); propofol: 22.2 (0.7), P<0.001 *vs* vehicle; propofol+CX546: 40.3 (1.2), P=0.059 *vs* vehicle, P<0.001 *vs* propofol; propofol+PTZ: 45.2 (1.1), P<0.001 *vs* vehicle, P<0.001 *vs* propofol; during running state, vehicle: 41.5 (0.9); propofol: 31.9 (0.7), P<0.001 *vs* vehicle; propofol+CX546: 41.5 (0.92), P=0.77 *vs* vehicle, P<0.001 *vs* propofol; propofol+PTZ: 44.4 (1.3), P=0.19 *vs* vehicle, P<0.001 *vs* propofol. For the product of Ca^{2+} activity and length of active dendritic segments during resting state, vehicle: 25.0 (0.9); propofol: 13.6 (0.50), P<0.001 *vs* vehicle; propofol+CX546: 26.2 (0.8), P=0.42 *vs* vehicle, P<0.001 *vs* propofol; propofol+PTZ: 29.0 (0.7), P<0.001 *vs* vehicle, P<0.001 *vs* propofol; during running state, vehicle: 57.4 (1.5); propofol: 36.6 (1.0), P<0.001 *vs* vehicle; propofol+CX546: 57.9 (1.5), P=0.75 *vs* vehicle, P<0.001 *vs* propofol; propofol+PTZ: 59.4 (1.96), P=0.20 *vs* vehicle, P<0.001 *vs* propofol. (e), (g), and (i) Distribution of Ca^{2+} activity on individual branches and length of active segment during resting and running (n=3–5 mice per group). Data are presented as mean (standard error of the mean). *P<0.05, **P<0.01, ***P<0.001. (d), (f), and (h) Kolmogorov–Smirnov's test. PTZ, pentylenetetrazol.

resting states (92.1% [2.6%] *vs* 121.8% [3.8%]; P<0.001) (Fig. 6l–p). Notably, motor-training-evoked activity in VIP neurones was increased in propofol-treated mice as compared with vehicle controls (448.4% [31.4%] *vs* 231.9% [10.6%]; P<0.001) (Fig. 6l–p), consistent with the connectivity scheme that VIP neurones inhibit SST and PV cells.

Taken together, these experiments indicate that repeated exposure to propofol during early postnatal life caused

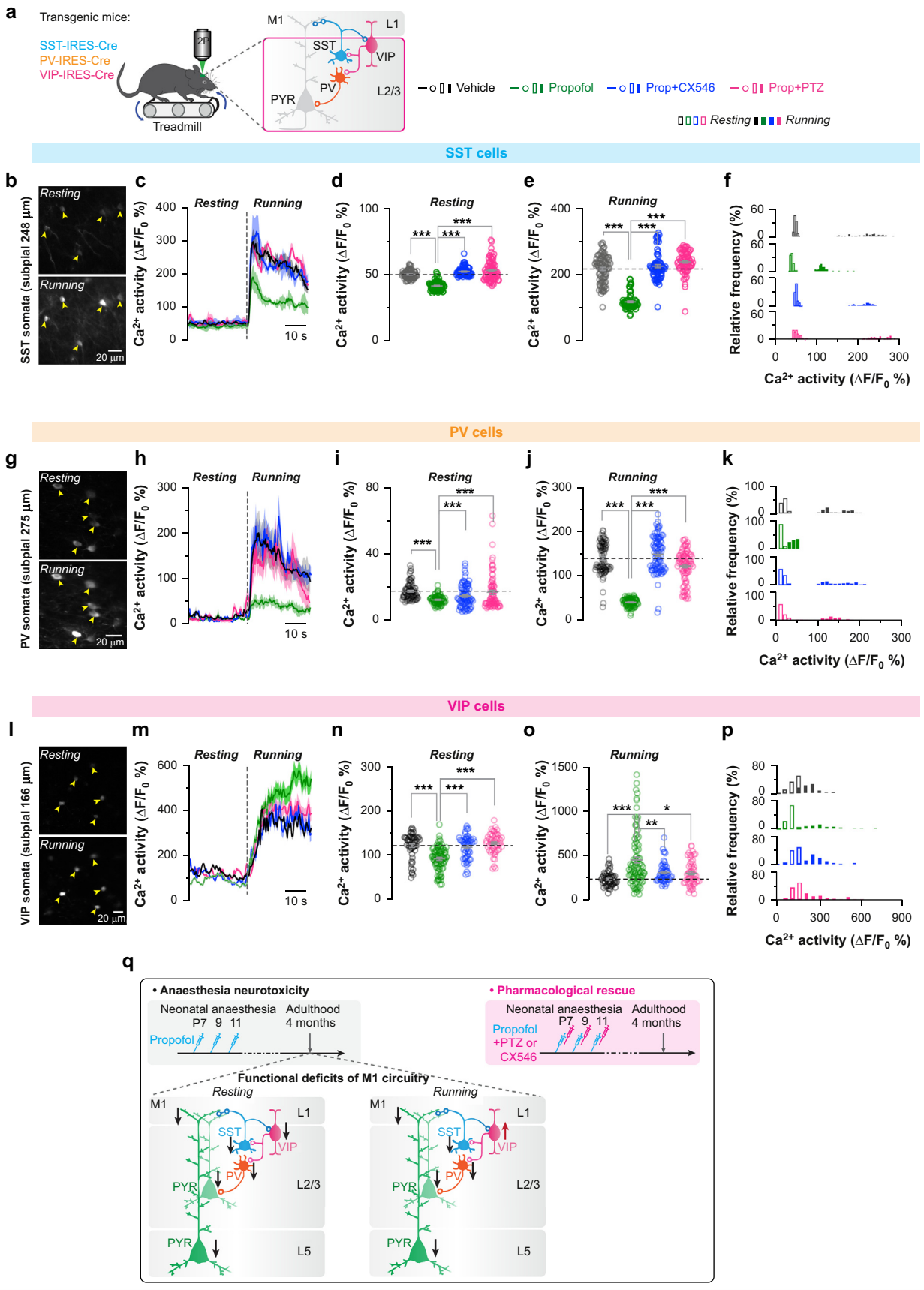
a
Transgenic mice:
SST-IRES-Cre
PV-IRES-Cre
VIP-IRES-Cre
2P
Treadmill
M1
L1
SST
VIP
PV
PYR
L2/3
Vehicle
Propofol
Prop+CX546
Prop+PTZ
Resting
Running
SST cells
b
SST somata (subpial 248 µm)
Resting
Running
20 µm
c
Ca2+ activity (ΔF/F0 %)
10 s
d
e
f
Relative frequency (%)
Ca2+ activity (ΔF/F0 %)
PV cells
g
PV somata (subpial 275 µm)
h
i
j
k
VIP cells
l
VIP somata (subpial 166 µm)
m
n
o
p
q
• Anaesthesia neurotoxicity
Neonatal anaesthesia
P7 9 11
Adulthood
4 months
Propofol
• Pharmacological rescue
Propofol
+PTZ or
CX546
Functional deficits of M1 circuitry
L5

persistent changes in SST, PV, and VIP interneurones in the cortex: spontaneous activity was decreased, whilst running-evoked activity was lower in SST and PV interneurones and higher in VIP interneurones, relative to vehicle-treated control mice. Mice administered PTZ or CX546 after propofol showed similar Ca^{2+} activity in SST-, PV-, and VIP-expressing interneurons as controls (Fig. 6b–p).

Discussion

How neonatal anaesthesia impairs neuronal circuit development, contributing to cognitive and behavioural deficits later in life, is poorly understood. In this study, we found that repeated exposure of mice to propofol anaesthesia during early postnatal development caused neuronal circuit dysfunction in the adult motor cortex (Fig. 6q). During the process of motor learning, task-associated activity was reduced in pyramidal neurones and in SST and PV interneurones. Potentiation of neuronal activity during post-anaesthesia recovery by PTZ or CX546 protected cortical network development and alleviated behavioural deficits.

Preclinical research has shown that anaesthetic neurotoxicity is dependent on the cumulative dose and duration of anaesthetic exposure.[17] Several well-designed human trials have studied whether the most common paediatric anaesthetics affect intelligence and other behavioural domains in healthy children.[49–51] Short exposures (<1 h) do not cause measurable decreases in general intelligence, consistent with findings in laboratory animals. It remains to be investigated whether repeated or prolonged exposure in young children, for example those undergoing extended and repeated surgery and those sedated for days in the neonatal ICU, may lead to behavioural and learning difficulties later in life. Nevertheless, it is imperative to understand the effects of clinically used anaesthetics and sedatives on brain development.

Propofol is used with increasing frequency for paediatric and obstetric procedures requiring anaesthesia or sedation. Propofol interacts with the β-subunit of the $GABA_A$ receptor to slow deactivation and desensitisation of the channel.[52] We found that a single dose of propofol anaesthetised P7 mice for less than 1 h, but suppressed neuronal activity in the cortex for more than 2 h, indicating a prolonged effect of propofol exposure on brain activity. Similar findings have been reported in young mice administered ketamine,[18] an anaesthetic that primarily blocks *N*-methyl-*D*-aspartate (NMDA) receptors. Together, these studies suggest that the impact of general anaesthetics on the developing brain may extend into the anaesthesia recovery period. Given the important role of neuronal activity in neural development, anaesthesia in the neonatal period may have long-lasting effects on neuronal circuits in the neocortex.

The motor cortex is known to control both simple and complex motor behaviours. Acquisition of motor skills involves activation of pyramidal neurones in both L2/3 and L5 of the primary motor cortex, and remodelling of spines on pyramidal neurone dendrites.[43,53–55] The number of dendritic spines formed and persisting after motor learning correlates with the degree of performance improvement in mice.[53,56] Many lines of evidence indicate that dendritic spikes contribute to synaptic plasticity.[44,45] Dendritic calcium spikes in apical dendrites of L5 pyramidal neurones are important for dendritic spine plasticity in the motor cortex.[43] By imaging apical tuft dendrites and somata of pyramidal neurones in the motor cortex, we found a substantial and persistent reduction in dendritic and somatic Ca^{2+} activity after repeated propofol anaesthesia. Moreover, both vGLUT1 and AMPAR expressions were reduced in the motor cortex, consistent with a decrease of excitatory synaptic input and function. Similar findings have been reported in neonatal mice after repeated ketamine anaesthesia.[18] Pyramidal neurone hypofunction after multiple anaesthetic doses may account for the reduction of learning-induced synaptic plasticity and motor learning impairments.[18]

Inhibitory circuits in the neocortex control and shape the activity of principal cells. Development of inhibitory circuits occurs later than excitatory circuits and is activity dependent.[57] Thus, early exposure to anaesthetics may not only have a significant impact on excitatory neurones, but also on the development of inhibitory circuits. Blockade of either glutamate receptors or $GABA_A$ receptors interferes with migration of GABAergic neurones,[58] and glutamate-mediated activity has an important role in the development of axons and dendrites of cortical inhibitory neurones *in vivo*.[59] *In vitro*,

Fig 6. Repeated neonatal propofol anaesthesia affects inhibitory interneurone activity that is rescued by PTZ or CX546 treatment. (a) Schematic of Ca^{2+} imaging of SST, PV, and VIP cells in L2/3 of the motor cortex during treadmill training. (b) Images of SST somata expressing GCaMP6s during resting and running. (c) Population average response of SST interneurones. Envelopes indicate standard error of the mean (SEM). (d) Measures of Ca^{2+} activity in SST neurones during resting. Vehicle: 50.6 (0.3); propofol: 42.0(0.4), $P<0.001$ *vs* vehicle; propofol+CX546: 52.7 (0.4), $P<0.001$ *vs* vehicle, $P<0.001$ *vs* propofol; propofol+PTZ: 53.7 (0.8), $P=0.001$ *vs* vehicle, $P<0.001$ *vs* propofol. (e) Measures of Ca^{2+} activity in SST neurones during running. Vehicle: 219.6 (4.3); propofol: 121.0 (2.7), $P<0.001$ *vs* vehicle; propofol+CX546: 227.6 (4.7), $P=0.18$ *vs* vehicle, $P<0.001$ *vs* propofol; propofol+PTZ: 240.8 (3.8), $P=0.003$ *vs* vehicle, $P<0.001$ *vs* propofol. (f) Distribution of Ca^{2+} activity in individual SST neurones during resting and running ($n=76–88$ cells from three to four mice per group). (g–k) Similar to (b–f), but in PV cells ($n=84–90$ cells from three to five mice per group). (i) Vehicle: 17.6 (0.5); propofol: 12.4 (0.3), $P<0.001$ *vs* vehicle; propofol+CX546: 14.9 (0.7), $P<0.001$ *vs* vehicle, $P<0.001$ *vs* propofol; propofol+PTZ: 17.0 (1.2), $P<0.001$ *vs* vehicle, $P=0.001$ *vs* propofol. (j) Vehicle: 139.5 (3.7); propofol: 40.5 (0.9), $P<0.001$ *vs* vehicle; propofol+CX546: 148.8 (4.2), $P=0.17$ *vs* vehicle, $P<0.001$ *vs* propofol; propofol+PTZ: 122.3 (3.8), $P=0.002$ *vs* vehicle, $P<0.001$ *vs* propofol. (l–p) Similar to (b–f), but in VIP cells ($n=52–95$ cells from three to five mice per group). (n) Vehicle: 121.8 (3.8); propofol: 92.1 (2.6), $P<0.001$ *vs* vehicle; propofol+CX546: 118.2 (3.6), $P=0.31$ *vs* vehicle, $P<0.001$ *vs* propofol; propofol+PTZ: 127.1 (3.2), $P=0.83$ *vs* vehicle, $P<0.001$ *vs* propofol. (o) Vehicle: 231.9 (10.6); propofol: 448.4 (31.4), $P<0.001$ *vs* vehicle; propofol+CX546: 306.1 (15.1), $P=0.001$ *vs* vehicle, $P=0.010$ *vs* propofol; propofol+PTZ: 299.9 (19.1), $P=0.010$ *vs* vehicle, $P=0.020$ *vs* propofol. Data are presented as mean (SEM) *$P<0.05$; **$P<0.01$; ***$P<0.001$; NS, not significant. (d, e, i, j, n, and o) Kolmogorov–Smirnov's test. (q) Schematic illustrating changes of neuronal circuits in the motor cortex after repeated neonatal anaesthesia. Four months after propofol exposures, spontaneous activities are low in both pyramidal (PYR) neurones and inhibitory interneurones (SST, PV, and VIP). During running, despite VIP activation, PYR neuronal activity remains low, which is associated with a decrease in excitatory synaptic inputs and generation of dendritic Ca^{2+} spikes. Administration of low-dose PTZ or CX546 after propofol ameliorates neuronal dysfunction in the cortex. M1, primary motor cortex. Up and down arrows indicate high and low activities, respectively, relative to vehicle-treated control mice. PTZ, pentylenetetrazol; PV, parvalbumin; SST, somatostatin; VIP, vasoactive intestinal polypeptide.

low concentrations of ketamine impair dendritic growth of immature GABAergic neurones and cause branch atrophy of differentiated GABAergic neurones.[22,23] We found a persistent reduction of spontaneous activity in three different subtypes of interneurones (SST, PV, and VIP) in the motor cortex after repeated propofol anaesthesia during P7–P11, indicating hypofunction of neuronal circuits in the motor cortex. In the cerebral cortex, a unique mode of inhibitory control is provided by VIP inhibitory neurones that specifically suppress the firing of other inhibitory neurones (SST and PV cells). Such disinhibition could lead to selective amplification of local processing and could provide gating and gain modulation.[48] We found that in propofol-treated mice, running-evoked activity in pyramidal neurones remained lower than in control mice despite increased VIP activation. Thus, early-life anaesthesia exposure induces lasting changes of neuronal activity in both excitatory pyramidal neurones and inhibitory interneurones.

Administration of the ampakine drug CX546 to potentiate AMPAR activity during emergence from ketamine anaesthesia restores neuronal activity and prevents long-term learning deficits induced by repeated neonatal exposure.[18] In line with the beneficial effects of ampakine for ketamine anaesthesia, we found that CX546 is also effective in protecting against the detrimental effects caused by propofol anaesthesia. These findings indicate that potentiation of AMPA function during anaesthesia recovery could offer neuroprotection to wide-ranging anaesthetics that target either NMDA or $GABA_A$ receptors in the CNS. Moreover, we found that systemic administration of PTZ to attenuate $GABA_A$ receptor activity in neonatal mice is also effective in promptly restoring brain activity after anaesthesia. Pentylenetetrazol is a non-competitive $GABA_A$ receptor antagonist. Previous studies have shown that chronic administration of low-dose non-competitive $GABA_A$ antagonists, including PTZ, ameliorates cognitive deficits in a mouse model of Down's syndrome that has excessive inhibition in the dentate gyrus.[41,60] We found that injections of PTZ after propofol expedited the recovery of neuronal activity in cortical pyramidal neurones. Importantly, mice treated with PTZ after propofol showed normal density of neurones, neuronal network activity, and behavioural performance. These findings corroborate the idea that pharmacologically enhancing neuronal activity during the anaesthesia recovery period could reduce the adverse effects of early-life anaesthesia.

There are several limitations in this study. First, *in vivo* two-photon Ca^{2+} imaging was performed on animals in head restraint. Because the awake, head-restraining situation may induce stress and potentially cause changes in neuronal activity, it is crucial to habituate animals to the imaging set-up before imaging to minimise stress. Second, the current study focused on motor learning and associated changes in excitatory and inhibitory neuronal activities in the motor cortex. Future studies of brain regions important for cognitive, social, and emotional development, such as hippocampus and prefrontal cortex, are needed to better understand the impact of general anaesthetics on neurodevelopment.

In summary, our data reveal long-lasting effects of general anaesthesia on cortical circuit development. Repeated exposure to propofol during early postnatal brain development caused a persistent reduction of cortical pyramidal neuronal activity and alterations of local inhibitory interneurone networks. Post-anaesthesia suppression of $GABA_A$ receptor activity or potentiation of AMPAR function prevented anaesthesia-induced learning and neuronal circuit deficits. Thus, prompt restoration of neuronal activity during recovery from anaesthesia is an effective strategy to reduce the adverse effects of early-life anaesthesia.

Authors' contributions

Experiment design: HZ, GY
Experimentation: HZ
Data analysis: HZ
Data interpretation: all authors
Writing of paper: all authors
Approval of version to be published: all authors

Acknowledgements

The authors thank Yang laboratory members for helpful discussions.

Declarations of interest

The authors declare that they have no conflicts of interest.

Funding

US National Institutes of Health (R35GM131765) to GY and (R01AG041274) to ZX and GY; Columbia University Medical Center Target of Opportunity Provost award to the Department of Anesthesiology.

Appendix A. Supplementary data

Supplementary data to this article can be found online at https://doi.org/10.1016/j.bja.2021.01.017.

References

1. Hubel DH, Wiesel TN. The period of susceptibility to the physiological effects of unilateral eye closure in kittens. *J Physiol* 1970; **206**: 419–36
2. Ackman JB, Burbridge TJ, Crair MC. Retinal waves coordinate patterned activity throughout the developing visual system. *Nature* 2012; **490**: 219–25
3. Ikonomidou C, Bittigau P, Ishimaru MJ, et al. Ethanol-induced apoptotic neurodegeneration and fetal alcohol syndrome. *Science* 2000; **287**: 1056–60
4. Rudolph U, Antkowiak B. Molecular and neuronal substrates for general anaesthetics. *Nat Rev Neurosci* 2004; **5**: 709–20
5. Hemmings Jr HC, Akabas MH, Goldstein PA, Trudell JR, Orser BA, Harrison NL. Emerging molecular mechanisms of general anesthetic action. *Trends Pharmacol Sci* 2005; **26**: 503–10
6. Vutskits L, Xie Z. Lasting impact of general anaesthesia on the brain: mechanisms and relevance. *Nat Rev Neurosci* 2016; **17**: 705–17
7. DiMaggio C, Sun LS, Kakavouli A, Byrne MW, Li G. A retrospective cohort study of the association of anesthesia and hernia repair surgery with behavioral and developmental disorders in young children. *J Neurosurg Anesthesiol* 2009; **21**: 286–91

8. Wilder RT, Flick RP, Sprung J, et al. Early exposure to anesthesia and learning disabilities in a population-based birth cohort. *Anesthesiology* 2009; **110**: 796–804
9. Ing C, DiMaggio C, Whitehouse A, et al. Long-term differences in language and cognitive function after childhood exposure to anesthesia. *Pediatrics* 2012; **130**: e476–85
10. Jevtovic-Todorovic V, Hartman RE, Izumi Y, et al. Early exposure to common anesthetic agents causes widespread neurodegeneration in the developing rat brain and persistent learning deficits. *J Neurosci* 2003; **23**: 876–82
11. Fredriksson A, Ponten E, Gordh T, Eriksson P. Neonatal exposure to a combination of N-methyl-D-aspartate and gamma-aminobutyric acid type A receptor anesthetic agents potentiates apoptotic neurodegeneration and persistent behavioral deficits. *Anesthesiology* 2007; **107**: 427–36
12. Brambrink AM, Evers AS, Avidan MS, et al. Isoflurane-induced neuroapoptosis in the neonatal rhesus macaque brain. *Anesthesiology* 2010; **112**: 834–41
13. Creeley C, Dikranian K, Dissen G, Martin L, Olney J, Brambrink A. Propofol-induced apoptosis of neurones and oligodendrocytes in fetal and neonatal rhesus macaque brain. *Br J Anaesth* 2013; **110**: i29–38
14. Kang E, Jiang D, Ryu YK, et al. Early postnatal exposure to isoflurane causes cognitive deficits and disrupts development of newborn hippocampal neurons via activation of the mTOR pathway. *PLoS Biol* 2017; **15**, e2001246
15. Zhou B, Chen L, Liao P, et al. Astroglial dysfunctions drive aberrant synaptogenesis and social behavioral deficits in mice with neonatal exposure to lengthy general anesthesia. *PLoS Biol* 2019; **17**, e3000086
16. Lunardi N, Sica R, Atluri N, et al. Disruption of rapid eye movement sleep homeostasis in adolescent rats after neonatal anesthesia. *Anesthesiology* 2019; **130**: 981–94
17. Coleman K, Robertson ND, Dissen GA, et al. Isoflurane anesthesia has long-term consequences on motor and behavioral development in infant rhesus macaques. *Anesthesiology* 2017; **126**: 74–84
18. Huang L, Cichon J, Ninan I, Yang G. Post-anesthesia AMPA receptor potentiation prevents anesthesia-induced learning and synaptic deficits. *Sci Transl Med* 2016; **8**: 344ra85
19. De Roo M, Klauser P, Briner A, et al. Anesthetics rapidly promote synaptogenesis during a critical period of brain development. *PLoS One* 2009; **4**, e7043
20. Briner A, Nikonenko I, De Roo M, Dayer A, Muller D, Vutskits L. Developmental stage-dependent persistent impact of propofol anesthesia on dendritic spines in the rat medial prefrontal cortex. *Anesthesiology* 2011; **115**: 282–93
21. Huang L, Yang G. Repeated exposure to ketamine-xylazine during early development impairs motor learning-dependent dendritic spine plasticity in adulthood. *Anesthesiology* 2015; **122**: 821–31
22. Vutskits L, Gascon E, Tassonyi E, Kiss JZ. Effect of ketamine on dendritic arbor development and survival of immature GABAergic neurons in vitro. *Toxicol Sci* 2006; **91**: 540–9
23. Vutskits L, Gascon E, Potter G, Tassonyi E, Kiss JZ. Low concentrations of ketamine initiate dendritic atrophy of differentiated GABAergic neurons in culture. *Toxicology* 2007; **234**: 216–26
24. Aligny C, Roux C, Dourmap N, et al. Ketamine alters cortical integration of GABAergic interneurons and induces long-term sex-dependent impairments in transgenic Gad67-GFP mice. *Cell Death Dis* 2014; **5**: e1311
25. Rudy B, Fishell G, Lee S, Hjerling-Leffler J. Three groups of interneurons account for nearly 100% of neocortical GABAergic neurons. *Dev Neurobiol* 2011; **71**: 45–61
26. Kepecs A, Fishell G. Interneuron cell types are fit to function. *Nature* 2014; **505**: 318–26
27. Banerjee P, Rossi MG, Anghelescu DL, et al. Association between anesthesia exposure and neurocognitive and neuroimaging outcomes in long-term survivors of childhood acute lymphoblastic leukemia. *JAMA Oncol* 2019; **5**: 1456–63
28. Cichon J, Magrane J, Shtridler E, et al. Imaging neuronal activity in the central and peripheral nervous systems using new *Thy1.2*-GCaMP6 transgenic mouse lines. *J Neurosci Methods* 2020; **334**: 108535
29. Cattano D, Young C, Straiko MM, Olney JW. Subanesthetic doses of propofol induce neuroapoptosis in the infant mouse brain. *Anesth Analg* 2008; **106**: 1712–4
30. Yang G, Pan F, Chang PC, Gooden F, Gan WB. Transcranial two-photon imaging of synaptic structures in the cortex of awake head-restrained mice. *Methods Mol Biol* 2013; **1010**: 35–43
31. Yang G, Pan F, Parkhurst CN, Grutzendler J, Gan WB. Thinned-skull cranial window technique for long-term imaging of the cortex in live mice. *Nat Protoc* 2010; **5**: 201–8
32. Cichon J, Blanck TJJ, Gan WB, Yang G. Activation of cortical somatostatin interneurons prevents the development of neuropathic pain. *Nat Neurosci* 2017; **20**: 1122–32
33. Adler A, Zhao R, Shin ME, Yasuda R, Gan WB. Somatostatin-expressing interneurons enable and maintain learning-dependent sequential activation of pyramidal neurons. *Neuron* 2019; **102**: 202–16. e7
34. Giovannucci A, Friedrich J, Gunn P, et al. CaImAn an open source tool for scalable calcium imaging data analysis. *eLife* 2019; **8**, e38173
35. Pnevmatikakis EA, Giovannucci A. NoRMCorre: an online algorithm for piecewise rigid motion correction of calcium imaging data. *J Neurosci Methods* 2017; **291**: 83–94
36. Pnevmatikakis EA, Soudry D, Gao Y, et al. Simultaneous denoising, deconvolution, and demixing of calcium imaging data. *Neuron* 2016; **89**: 285–99
37. Vogelstein JT, Packer AM, Machado TA, et al. Fast nonnegative deconvolution for spike train inference from population calcium imaging. *J Neurophysiol* 2010; **104**: 3691–704
38. Huang L, Hayes S, Yang G. Long-lasting behavioral effects in neonatal mice with multiple exposures to ketamine-xylazine anesthesia. *Neurotoxicol Teratol* 2017; **60**: 75–81
39. Bourgeois T, Ringot M, Ramanantsoa N, et al. Breathing under anesthesia: a key role for the retrotrapezoid nucleus revealed by conditional Phox2b mutant mice. *Anesthesiology* 2019; **130**: 995–1006
40. Irifune M, Takarada T, Shimizu Y, et al. Propofol-induced anesthesia in mice is mediated by gamma-aminobutyric acid-A and excitatory amino acid receptors. *Anesth Analg* 2003; **97**: 424–9 [table of contents]
41. Colas D, Chuluun B, Warrier D, et al. Short-term treatment with the $GABA_A$ receptor antagonist pentylenetetrazole produces a sustained pro-cognitive benefit in a mouse model of Down's syndrome. *Br J Pharmacol* 2013; **169**: 963–73
42. Huang RQ, Bell-Horner CL, Dibas MI, Covey DF, Drewe JA, Dillon GH. Pentylenetetrazole-induced inhibition of

recombinant gamma-aminobutyric acid type A (GABA(A)) receptors: mechanism and site of action. *J Pharmacol Exp Ther* 2001; **298**: 986–95
43. Cichon J, Gan WB. Branch-specific dendritic Ca^{2+} spikes cause persistent synaptic plasticity. *Nature* 2015; **520**: 180–5
44. Golding NL, Staff NP, Spruston N. Dendritic spikes as a mechanism for cooperative long-term potentiation. *Nature* 2002; **418**: 326–31
45. Humeau Y, Luthi A. Dendritic calcium spikes induce bidirectional synaptic plasticity in the lateral amygdala. *Neuropharmacology* 2007; **52**: 234–43
46. Chiu CQ, Lur G, Morse TM, Carnevale NT, Ellis-Davies GC, Higley MJ. Compartmentalization of GABAergic inhibition by dendritic spines. *Science* 2013; **340**: 759–62
47. Marlin JJ, Carter AG. GABA-A receptor inhibition of local calcium signaling in spines and dendrites. *J Neurosci* 2014; **34**: 15898–911
48. Pi HJ, Hangya B, Kvitsiani D, Sanders JI, Huang ZJ, Kepecs A. Cortical interneurons that specialize in disinhibitory control. *Nature* 2013; **503**: 521–4
49. Warner DO, Zaccariello MJ, Katusic SK, et al. Neuropsychological and behavioral outcomes after exposure of young children to procedures requiring general anesthesia: the Mayo Anesthesia Safety in Kids (MASK) study. *Anesthesiology* 2018; **129**: 89–105
50. Sun LS, Li G, Miller TL, et al. Association between a single general anesthesia exposure before age 36 months and neurocognitive outcomes in later childhood. *JAMA* 2016; **315**: 2312–20
51. McCann ME, de Graaff JC, Dorris L, et al. Neurodevelopmental outcome at 5 years of age after general anaesthesia or awake-regional anaesthesia in infancy (GAS): an international, multicentre, randomised, controlled equivalence trial. *Lancet* 2019; **393**: 664–77
52. Bai D, Pennefather PS, MacDonald JF, Orser BA. The general anesthetic propofol slows deactivation and desensitization of $GABA_A$ receptors. *J Neurosci* 1999; **19**: 10635–46
53. Yang G, Pan F, Gan WB. Stably maintained dendritic spines are associated with lifelong memories. *Nature* 2009; **462**: 920–4
54. Yang G, Lai CS, Cichon J, Ma L, Li W, Gan WB. Sleep promotes branch-specific formation of dendritic spines after learning. *Science* 2014; **344**: 1173–8
55. Ma L, Qiao Q, Tsai JW, Yang G, Li W, Gan WB. Experience-dependent plasticity of dendritic spines of layer 2/3 pyramidal neurons in the mouse cortex. *Dev Neurobiol* 2016; **76**: 277–86
56. Liston C, Cichon JM, Jeanneteau F, Jia Z, Chao MV, Gan WB. Circadian glucocorticoid oscillations promote learning-dependent synapse formation and maintenance. *Nat Neurosci* 2013; **16**: 698–705
57. Lim L, Mi D, Llorca A, Marin O. Development and functional diversification of cortical interneurons. *Neuron* 2018; **100**: 294–313
58. De Marco Garcia NV, Karayannis T, Fishell G. Neuronal activity is required for the development of specific cortical interneuron subtypes. *Nature* 2011; **472**: 351–5
59. de Lima AD, Gieseler A, Voigt T. Relationship between GABAergic interneurons migration and early neocortical network activity. *Dev Neurobiol* 2009; **69**: 105–23
60. Fernandez F, Morishita W, Zuniga E, et al. Pharmacotherapy for cognitive impairment in a mouse model of Down syndrome. *Nat Neurosci* 2007; **10**: 411–3

Handling editor: Hugh C Hemmings Jr